

group, that are concerned with segmental identity, leading to a view of evolution in which most animals evolved from a segmented animal with a relatively complex anatomy. This view has been challenged, however, not least by work on enteropneusts showing that anatomy is no guide to the complexity of gene expression⁵. *Xenoturbella* could be a model of early deuterostome ancestry, if not the ancestry of both deuterostomes and protostomes. Classifying it as a flatworm, therefore, might not have been so far from the truth, as that is what the earliest deuterostomes may have looked like.

However, the fact that Bourlat and colleagues³ have placed *Xenoturbella* closer to the ambulacraria than to the root of deuterostomes in general raises further problems, for it means that it cannot represent a truly primitive state. Ambulacraria and chordates share anatomical features, such as a body cavity and structures called pharyngeal slits,

that were presumably primitively present in the *Xenoturbella* lineage but have since been lost. This means that *Xenoturbella* is secondarily simplified rather than pristine and primitive, and may not be as reliable a guide to deuterostome evolution as we should like.

As we reflect on *Xenoturbella*'s newly exalted state as a deuterostome, it is worth recalling similar examples. Aristotle classed tunicates with the molluscs, and the amphioxus, when first described, was named *Limax lanceolatus* — a kind of slug. So there is no shame in having once been classed as a mollusc: many of the best deuterostomes started out that way. ■

Henry Gee is a senior editor at Nature.

1. Norén, M. & Jondelius, U. *Nature* **390**, 31–32 (1997).
2. Israelsson, O. *Nature* **390**, 32 (1997).
3. Bourlat, S. J., Nielsen, C., Lockyer, A. E., Littlewood, D. T. J. & Telford, M. J. *Nature* **424**, 925–928 (2003).
4. Shu, D.-G. *et al.* *Nature* **414**, 419–424 (2001).
5. Lowe, C. J. *et al.* *Cell* **113**, 853–865 (2003).

Granular materials

Shaken sand — a granular fluid?

Paul Umbanhowar

The connection between random grain motion and viscosity in shaken sand — a strongly non-equilibrium system — has been probed. Curiously, the link is similar to that found in an ordinary liquid in thermal equilibrium.

By measuring both the free and forced oscillations of a rigid pendulum immersed in an ordinary liquid, the temperature and viscosity of the liquid can be determined¹. This is due, in part, to a relation from equilibrium statistical mechanics known as the fluctuation–dissipation theorem², which, in a precursor to its modern form, was devised by Einstein³ to explain the diffusive Brownian motion of small particles suspended in liquids⁴. Driven granular materials, such as shaken sand, are systems far from equilibrium — they have strong spatial and temporal variations in quantities such as density and local particle velocity, and would consequently not be expected to obey the fluctuation–dissipation theorem.

Yet, in many instances, the macroscopic behaviour of granular materials seems, at least superficially, liquid-like⁵. One might then wonder whether an experiment using a rigid pendulum would reveal a similar fluctuation–dissipation relation in driven granular materials, despite their dissipative nature. On page 909 of this issue⁶, D'Anna and colleagues take up this question and find, surprisingly, that the answer seems to be yes. In particular, their experiments show that the free and forced motions of the probe are related by a fluctuation–dissipation-like relation, and that an effective viscosity and temperature can be defined.

Granular materials — such as peas, coal,

pillars, breakfast cereal and, not least of all, sand — are usually defined to be discrete solid bits that interact with each other through energy-dissipating contact forces (although the definition is sometimes stretched to include wetted grains and powders for which attractive surface forces are also important). Many industrial practices require the efficient handling and mixing of granular materials: food and agricultural processing, sorting and assembly of parts, cement manufacturing, mining, radiation shielding and, of ever increasing scope, pharmaceutical production. Despite their somewhat humble nature, granular materials behave unusually because they combine properties of both liquids and solids^{7,8}. Examples of such behaviour include the ability to de-mix when poured⁹, to form waves or ripples when shaken¹⁰ or blown¹¹, and to expand when squeezed¹² (as anyone can attest who has walked on wet sand and observed a dry halo around their foot).

Many of the unique properties of granular materials arise because, unlike an ordinary fluid, the kinetic energy associated with the relative motion of macroscopic particles (called 'granular temperature' by physicists) is not constant. Instead, it is continually and irrevocably transferred by collisions to internal (thermal or non-kinetic) degrees of freedom. Although individual grains possess a well-defined thermodynamic temperature,

the associated thermal energy (equal to the product kT , where k is Boltzmann's constant and T is the temperature in kelvin) is too small to allow relative particle motion, as it does in ordinary liquids. So dynamic collections of grains require a continuous external source of energy to prevent them from getting stuck in a particular configuration.

To complicate matters further, because energy is typically injected through a surface (a stirring rod, shear zone or vibrating wall, for example), steep gradients of kinetic energy are invariably present in the system, caused by the decrease in relative particle motion further from the energy source and by the spatial anisotropies arising from the directional nature of the forcing. These complications make it unclear whether granular liquids can be described by the traditional hydrodynamics derived from equilibrium statistical mechanics^{5,7,8}. And they are the major reasons why granular materials remain one of the least well understood classes of matter.

Rather than being deterred by the complications associated with the lack of energy conservation in granular media, D'Anna *et al.*⁶ have attacked the problem directly by studying the response of vertically vibrated glass beads (physicists' equivalent of sand), using a beefed-up version of the aforementioned pendulum (pictured on the cover of this issue). Their bead-filled container is driven with band-filtered white noise at a relatively high frequency, which ensures that no single characteristic frequency dominates the forcing, that the natural frequency of the oscillator is far below the driving frequency, and that the beads are condensed. The pendulum probe is operated in two modes: free and forced. In the free mode, a constant barrage of grains bombards the probe and jostles it about in irregular excursions about its equilibrium position. Analysis of this Brownian-like motion gives the 'noise power spectral density' in terms of the driving frequency. In the forced mode, a sinusoidal torque is applied to the oscillator, and measurements of the relative phase and amplitude of the response determine the 'complex susceptibility'.

Interestingly, the group finds that the measured complex susceptibility is well described by the theory developed for equilibrium fluids — one of the two parameters used in the fit to theory being the friction coefficient, which is proportional to the shaken beads' viscosity. Furthermore, the bead viscosity is found to decrease nearly linearly with increasing amplitude of shaking. Ordinary liquids show a similar decrease in viscosity with increasing temperature — nearly a factor of three for water between 0 °C and 45 °C.

Of greater interest is D'Anna and colleagues' finding⁶ concerning the so-called fluctuation–dissipation ratio, which is

derived from the complex susceptibility and the noise power spectral density, and so relates collective response to individual grain motion. This ratio turns out to be nearly constant for varying frequency, which enables D'Anna *et al.* to define an effective temperature for the grains. For a classical liquid, this ratio is equal to kT and is strictly independent of frequency. Using the average value of the ratio as their measure of thermal energy, the authors show that the temperature increases as the square of the driving-force amplitude — a result that would be naively expected if the bead velocities were linearly related to the container velocity, which in turn increases in direct proportion to the drive amplitude. These findings are intriguing, and they support results from other analyses of model systems that have indicated that the fluctuation–dissipation theorem, or a slightly modified version of it, applies to granular materials^{13–15}. There are also signs that the temperatures obtained through application of the fluctuation–dissipation theorem¹³ are compatible with the temperature obtained from a new form of statistical mechanics that is applicable to granular systems and possibly to other non-energy-conserving systems¹⁶.

D'Anna and colleagues' findings that granular ensembles with strong dissipation have a definable viscosity and approximately obey the fluctuation–dissipation theorem are exciting, but they do not yet definitively answer the question of how deep the similarities run between moving grains and ordinary

liquids. Some puzzles remain. Why does the effective temperature vary by approximately a factor of 10 for differently shaped probes? What influence does the probe have on the measurements? Why is the fluctuation–dissipation ratio an increasing function of frequency (albeit slowly)? The answers themselves may be mundane, but they might lead to deeper insights into the properties of granular materials and other related non-equilibrium subjects such as traffic flow, flocking, evolving networks and turbulence¹⁴. ■

Paul Umbanhowar is in the Department of Physics and Astronomy, Northwestern University,

2145 Sheridan Road, Evanston,

Illinois 60208–3112, USA.

e-mail: umbanhowar@nwu.edu

- Uhlenbeck, G. E. & Goudsmit, S. *Phys. Rev.* **34**, 145–151 (1929).
- Reichl, L. E. *A Modern Course in Statistical Physics* 545–560 (Univ. Texas Press, Austin, 1991).
- Einstein, A. *Ann. Physik* **17**, 549–560 (1905).
- Brown, R. *Phil. Mag.* **4**, 161–173 (1828).
- Jaeger, H. M., Nagel, S. R. & Behringer, R. P. *Rev. Mod. Phys.* **68**, 1259–1273 (1996).
- D'Anna, G., Mayor, P., Barrat, A., Loreto, V. & Nori, F. *Nature* **424**, 909–912 (2003).
- Kadanoff, L. P. *Rev. Mod. Phys.* **71**, 435–444 (1999).
- de Gennes, P. G. *Rev. Mod. Phys.* **71**, S374–S382 (1999).
- Makse, H. A., Havlin, S., King, P. R. & Stanley, H. E. *Nature* **386**, 379–382 (1997).
- Melo, F., Umbanhowar, P. B. & Swinney, H. L. *Phys. Rev. Lett.* **75**, 3838–3841 (1995).
- Bagnold, R. A. *The Physics of Blown Sand and Desert Dunes* (Methuen, London, 1941).
- Reynolds, O. *Phil. Mag.* **20**, 469 (1885).
- Makse, H. A. & Kurchan, J. *Nature* **415**, 614–617 (2002).
- Aumaitre, S., Fauve, S., McNamara, S. & Poggi, P. *Eur. Phys. J. B* **19**, 449–460 (2001).
- Colizza, V., Barrat, A. & Loreto, V. *Phys. Rev. E* **65**, 050301(R) (2002).
- Edwards, S. F. in *Granular Matter: An Interdisciplinary Approach* (ed. Mehta, A.) 121–140 (Springer, New York, 1994).

the two drugs most commonly used to treat malaria⁴. Hope for the containment of the disease now rests largely on a remarkable set of artemisinin drugs developed by Chinese scientists in the 1970s and early 1980s, which rapidly kill the malaria parasites.

The parasites are small 'protozoan' cells (the most prevalent species infecting humans are *Plasmodium falciparum* and *P. vivax*), which enter their human host through a mosquito bite. They first invade the liver and replicate there for two weeks, before beginning a cycle of red-blood-cell invasion, then growth, replication and red-cell destruction that leads to the disease symptoms. The artemisinin drugs are known to act specifically during this blood stage.

Artemisinin contains a structural feature called a peroxide bridge (Fig. 1), and this is believed to be the key to the drug's mode of action. Ferrous iron (Fe^{2+}) catalyses the cleavage of this bridge, forming highly reactive free radicals⁵. The theory has been that these artemisinin-derived free radicals chemically modify and inhibit a variety of parasite molecules, resulting in parasite death^{5,6}.

A rich source of intracellular Fe^{2+} is haem — an essential component of haemoglobin — and it has long been suspected that Fe^{2+} -haem is responsible for activating artemisinins inside the parasite. In support of this, Fe^{2+} -haem activates artemisinins in the test tube and haem–artemisinin complexes can be formed. This theory appealed to malariologists because it seemed to explain the specificity of the drug within the context of a unique aspect of parasite metabolism. During its growth and replication inside the red blood cell, the parasite ingests and degrades up to 80% of host-cell haemoglobin in a compartment called a food vacuole. This releases Fe^{2+} -haem, which is oxidized to Fe^{3+} -haematin and then aggregates within the food vacuole into an ordered crystalline pigment called haemozoin. A theory developed that the specific antimalarial effect of artemisinin was due to its entry into the parasite food vacuole and its interaction with Fe^{2+} -haem. Here, it would set off a 'cluster bomb' of free radicals, inhibiting several key parasite components and eventually resulting in parasite death.

This theory has been challenged⁷, however,

Malaria

To kill a parasite

Robert G. Ridley

Artemisinins have been used since ancient times to treat malaria. A new theory could explain how this age-old medicine is able to cause the death of the malaria parasite.

The Chinese herb qinghao (*Artemisia annua*) has long been used to treat malaria — Taoist manuscripts dating back to the third century describe the use of qinghao extracts to treat malaria-related fevers¹. Over the past two decades, derivatives of the herb's active ingredient, artemisinin, have made an increasing contribution to malaria treatment. But the precise mechanism by which artemisinin derivatives kill the parasite has remained obscure. Writing on page 957 of this issue, Krishna and colleagues² propose a radical new theory to explain the molecular basis of the antimalarial activity of artemisinin.

Malaria remains a scourge of the developing world, killing over a million people each year and infecting around 500 million³. Most of the victims are children under the age of

five living in sub-Saharan Africa, but the disease also afflicts Southeast Asia, South America and the Indian subcontinent. The situation has worsened over recent years as resistance has developed against chloroquine and sulphadoxine–pyrimethamine,

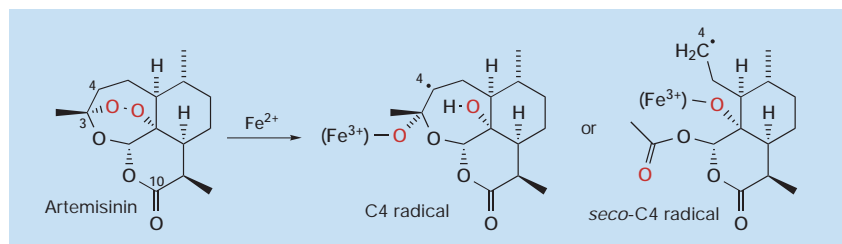


Figure 1 Structure of artemisinin. The molecule contains a peroxide bridge (red), which becomes cleaved when artemisinin interacts with ferrous iron (Fe^{2+}). Cleavage creates 'C4' and 'seco-C4' free radicals, each capable of chemically modifying biological molecules.

Think outside the sandbox

One grain of sand is a solid. But a lot of grains together can behave like a solid or a liquid. By probing this dual personality, physicists hope to understand a host of real-world systems, says Mark Buchanan.

Heinrich Jaeger knows what it's like, literally and metaphorically, to watch the sand slipping through the hourglass. "We thought it would be a four-week experiment," the physicist recalls of one of his studies. "It ended up taking several years."

A decade ago, Jaeger and his colleagues at the University of Chicago were busy studying what happened when they poured sand into a container and tapped the box repeatedly. They expected the grains to bed down fairly quickly — but, as the team eventually reported in 1995, the sand kept shifting into ever more compact configurations¹. "Granular systems look deceptively simple," says Jaeger. "But the closer we look, we find so many complexities."

Such puzzles show why granular materials hold a special fascination for physicists interested in the fundamental properties of matter. A pile of sand, flour or mustard seed can stand tall and fixed like a solid, defying the tug of gravity that would bring water sloshing to the floor. Yet sand pours through an hourglass as though it were a liquid.

People spend more time and effort in handling granular matter than any type of material aside from water. In industry, powders clog chutes and otherwise misbehave, at enormous economic expense. So understanding how simple forces — mostly gravity and friction — help to shape the materials' multiple personalities is of immense practical significance.

Out of equilibrium

What's more, some physicists believe that progress towards a theory of granular matter could provide clues to the wider world of 'non-equilibrium' physics. This is a large missing piece of the theoretical framework that physicists use to describe matter, and applies to the vast majority of real-world systems, which are not held in fixed and unchanging conditions but instead are shaken, stirred, heated, or driven by energy in countless other ways.

Theorists have long approached granular matter by considering it to be analogous to ordinary matter, with the grains playing the roles of individual molecules². At rest, a pile of grains is indeed rather like a solid, able to resist a certain amount of stress. But if you shake it vigorously, letting the grains tumble past one another and rearrange themselves, it does appear to shift into a



Stick or slick? Sand can be sculpted into solid forms, both by humans (above) and by the elements (above right). But put it in an hourglass and it flows like a liquid — and theorists want to know why.

'liquid' form. Much theorizing about the behaviour of granular matter therefore centres on the extent to which it is meaningful to talk about 'melting' piles of sand, and whether the degree of shaking might be related to an 'effective temperature' of the granular liquid.

Recent experimental results have revealed some fundamental similarities between granular liquids and their conventional counterparts. High-school physics students are familiar with the concept of brownian motion, in which a small particle floating in a pool of liquid dances around, driven by the thermal motions of the surrounding molecules. And Albert Einstein showed that the speed with which the particle wanders is linked to how easily the same particle can be dragged through the liquid by an external force³. Two numbers — a 'diffusion coefficient', D , and a 'mobility', μ — describe these two behaviours, and their ratio is always equal to the temperature of the liquid, T .

In August this year, Gianfranco D'Anna and his colleagues at the Swiss Federal Poly-

technic in Lausanne showed that this relationship also holds true for granular liquids⁴. They put 50,000 glass beads in a small container, which they vibrated at high frequency to generate 'liquid' behaviour. The team used this set-up to run a simplified version of Einstein's experiment: whereas he considered a particle that could wander freely, the cone-shaped 'particle' used by D'Anna's team was able only to rotate.

Go with the flow

Whatever the size of the cone, the ratio between D and μ was constant. And this effective temperature seemed to reflect accurately the vigour of the disordered motion of the constituent particles — just as a thermal temperature does for an ordinary liquid. "A granular liquid is indeed a fairly good liquid," says D'Anna.

The team's results lend support to the idea that granular matter is not such a misfit after all. They also raise an obvious question: if adequate vibration generates a liquid, what happens if the vibration is less strong? Weaker vibration corresponds to a lower

move, but with great difficulty. Because these structural rearrangements occur so slowly, the material is stable for most practical purposes. However, the physical properties of the glass — such as its electrical conductivity — gradually change as its structure evolves. Ordinary matter in equilibrium does not experience this sort of ‘ageing’.

Since Jaeger’s team reported its first results, theories developed to describe both granular solids and glassy materials have begun to converge — suggesting that the two types of matter are fundamentally similar.

Grains of truth

In the late 1980s, Sam Edwards of the University of Cambridge, UK, tried to formulate a theory of granular matter for one special case — a dense collection of grains flowing just fast enough to avoid sticking. For this regime, Edwards proposed that an accurate theory could be devised by supposing that the grains are equally likely to fall into any of the possible ‘jammed’ configurations⁵.

At the time, most physicists were unconvinced by the theory — it seemed possible, if not likely, that some of the jammed configurations would be more probable than others. “It was a very bold proposal,” says Jorge Kurchan of the Ecole Supérieure de Physique et de Chimie Industrielles in Paris. “Few took it very seriously.” A theory as simple as Edwards’, physicists reasoned, was unlikely to explain the complexities of granular behaviour.

By the late 1990s, however, Kurchan and other theorists were developing ways to understand ageing in glasses in fundamental terms⁶ — and their theories bore a striking resemblance to Edwards’ theory of granular matter. “In retrospect, his ideas were not so crazy after all,” says Kurchan.

Last year, Kurchan teamed up with Hernán Makse of the City College of New York to test Edwards’ ideas directly. Using a computer, they simulated the flow of grains trapped between a fixed lower surface and an upper surface moving just fast enough to keep the grains flowing. Like D’Anna and his colleagues, Kurchan and Makse measured the effective temperature of the grains by examining the relationship between D and μ for a simulated probe particle. Kurchan and Makse also calculated the effective temperature using Edwards’ theory, and found that the two results matched⁷.

Nonetheless, a full theory of granular matter remains some way off. As Kurchan points out, Edwards’ ideas do not apply to

granular liquids, in which the grains leave their jammed configurations behind. And some physicists wonder about the utility of the ‘effective temperature’ concept. “It is not clear,” says Douglas Durian of the University of California, Los Angeles, “if these temperatures have a predictive significance.” In earlier experiments, for example, effective temperatures measured for different types of flow tended to have different values, whereas a truly fundamental temperature should give the same value no matter how it is measured.

But the fact that some of the same fundamental ideas seem to apply to both granular matter and glassy materials is encouraging, as both are examples of non-equilibrium systems — and gaining a general understanding of these systems is near the top of the ‘to do’ list for theoretical physicists.

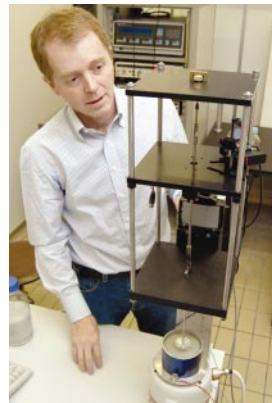
Current theories of solids, liquids and gases are based on equilibrium statistical mechanics, which apply only to systems that are in thermal equilibrium. A bowl of water at room temperature is one such system, as it has the same temperature as its surroundings. But a granular liquid is not in equilibrium — it needs a constant input of vibrational energy to retain its ‘liquid’ state. A ‘jammed’ granular system is also out of equilibrium, as the grains cannot easily explore all configurations. Similarly, the way in which the character of glass evolves with time is a direct consequence of the system having excess energy and taking an

incredibly long time to reach equilibrium.

The problem, for physicists interested in the fundamental behaviour of matter, is that most real-world systems are not in equilibrium. From the chemistry of living cells to the river of cars on a crowded highway, the real world is out of balance, perpetually flowing and evolving. If the recent surge of interest in granular matter leads to a deeper understanding of non-equilibrium systems in general, the theoretical pickings could be rich indeed. “Intellectually,” says Jaeger, “things are beginning to gel.” ■

Mark Buchanan is a freelance writer based in Cambridge, UK.

1. Knight, J. B., Fandrich, C. G., Lau, C. N., Jaeger, H. M. & Nagel, S. R. *Phys. Rev. E* **51**, 3957–3963 (1995).
2. Jaeger, H. M., Nagel, S. R. & Behringer, R. P. *Rev. Mod. Phys.* **68**, 1259–1273 (1996).
3. Einstein, A. *Ann. Physik* **17**, 549–560 (1905).
4. D’Anna, G., Mayor, P., Barrat, A., Loreto, V. & Nori, F. *Nature* **424**, 909–912 (2003).
5. Mehta, A. & Edwards, S. F. *Physica A* **157**, 1091–1097 (1989).
6. Cugliandolo, L. F., Kurchan, J. & Peliti, L. *Phys. Rev. E* **55**, 3898–3914 (1997).
7. Makse, H. A. & Kurchan, J. *Nature* **415**, 614–616 (2002).



Gianfranco D’Anna has studied the physics of ‘granular liquids’.

effective temperature. So, by analogy, a progressively less vigorously shaken granular liquid should reach a point at which it ‘freezes’ into a solid.

These are the conditions explored by Jaeger and his colleagues in their studies during the early 1990s. But their grains did not freeze into anything like an ordinary solid. Contrary to expectations, a few days of tapping did not bring the container of sand into a fully compact state. In some cases, the grains remained unsettled even after several hundred thousand taps¹. As Jaeger’s group suggested, this is similar to the way in which glassy materials solidify.

Upon cooling, the molecules of a glassy material do not fall into a regular, crystalline arrangement, but instead become jammed in a disordered structure. The molecules still

Getting to the bottom of a granular medium

A surprising resistance would be put up by sand grains hiding a buried treasure chest.

Penetration by an object through a dense granular medium (for example, by a finger pushing slowly into the sand on a beach) presents an interesting physics problem¹ that is closely related to issues of practical importance in soil science^{2,3}. Here we measure the penetration-resistance force for an object approaching the solid bottom boundary of a granular sample — analogous to the finger approaching a flat rock buried in the beach. We find that the penetration resistance near the boundary increases exponentially, which demonstrates the existence of an intrinsic length scale to the ‘jamming’ caused by a locally applied stress.

Our experimental apparatus consists of an actuator that pushes a flat circular plate of radius r vertically into a bucket of spherical glass beads filled to a depth of z_{\max} (see Supplementary Information). To obtain constant packing throughout the sample, we filled the bucket through a tube centred in the bucket and slowly raised the tube from the bottom⁴. An in-line force cell measured the penetration force, F , as a function of the height, z , of the plate’s surface above the bottom of the bucket. The penetration force was independent of the velocity for $0.0625 \leq v \leq 2.0 \text{ mm s}^{-1}$, as expected at such low velocities⁵.

Typical measurements of $F(z)$ are shown in Fig. 1a. Far from the bottom, we expect $F(z)$ to be proportional to the ambient granular pressure, and indeed $F(z)$ is roughly linear just below the top surface (that is, for $z \approx z_{\max}$) and begins to saturate when the plate is well below the surface (as expected, because the walls bear some of the weight of the grains³). We label this intrinsic depth dependence of the penetration force (the force that is not affected by the presence of the bottom boundary) as $F_{\text{bulk}}(z)$. The effect of the bottom boundary of the bucket is apparent in Fig. 1a as a rapid increase in $F(z)$ as $z \rightarrow 0$.

To separate the effect of the bottom boundary on $F(z)$ from the intrinsic depth dependence of the penetration force in bulk material, $F_{\text{bulk}}(z)$, we acquired the functional form of $F_{\text{bulk}}(z)$ by measuring the penetration force in a bucket filled sufficiently to prevent the plate from ever approaching the bottom. As shown in Fig. 1a, by translating these data to account for different values of z_{\max} , we can obtain $F_{\text{bulk}}(z)$ for any value of z_{\max} . These results are not affected by the bottom boundary, so they provide a background measurement of the penetration force. By taking the difference between this background and the measured penetration force, we obtain the differential penetration force

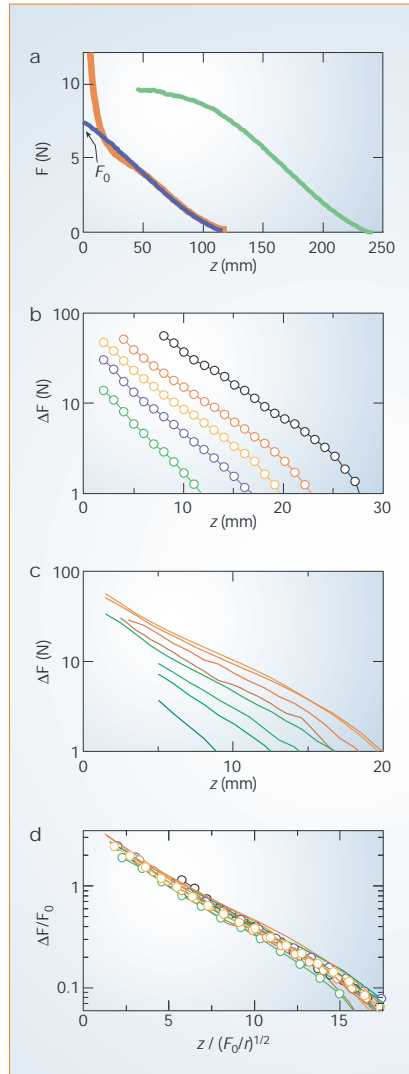


Figure 1 Penetration effects of an object approaching the solid bottom boundary of a granular sample. **a**, The penetration force, $F(z)$, for $z_{\max} = 112 \text{ mm}$ (red curve) and $z_{\max} = 230 \text{ mm}$ (green curve) was achieved by using a penetrating plate of 9.5 mm radius. $F_{\text{bulk}}(z)$ for $z_{\max} = 112 \text{ mm}$ (blue curve) was obtained by translating the $F(z)$ data acquired with $z_{\max} = 230 \text{ mm}$ so that they align with $F(z)$ data acquired with $z_{\max} = 112 \text{ mm}$. The location of F_0 , the value of $F_{\text{bulk}}(z)$ at $z=0$, is also indicated. Note also that $F(z) < F_{\text{bulk}}(z)$ for a small regime near the bottom boundary because grains slip near the smooth bottom boundary (this effect can be altered by the bottom surface texture). All data were obtained by using monodisperse spherical glass beads (Jaygo), where $d_{\text{grain}} = 0.92 \pm 0.03 \text{ mm}$. **b**, The differential penetration force, $\Delta F(z)$, for $z_{\max} = 112 \text{ mm}$ for plate radii of 9.5, 12.7, 15.9, 19.1 and 25.4 mm (from left to right). **c**, The differential penetration force, $\Delta F(z)$, for fill heights z_{\max} of 62, 82, 101, 116, 138, 153, 174 and 193 mm (from left to right along bottom) for a plate of radius $r = 12.7 \text{ mm}$. **d**, Scaled differential penetration force (see text) for data in **b** and **c**. The behaviour was exponential for rough and smooth bottom surfaces and for spherical grains as well as non-spherical sand.

$\Delta F(z) = F(z) - F_{\text{bulk}}(z)$, which quantifies the effect of the bottom surface.

Figure 1b, c shows the behaviour of $\Delta F(z)$ as the plate approaches the bottom of the bucket (that is, as $z \rightarrow 0$) for measurements varying the plate radius, r , and fill height, z_{\max} , respectively. The linear character of these semi-logarithmic plots indicates that $\Delta F(z)$ near the bottom is described by an exponential form, $\Delta F(z) \propto e^{-z/\lambda}$, which implies that λ is a characteristic length scale for sensing the bottom of the bucket ($\lambda \approx 5 \text{ mm}$, and is independent of grain diameter for d values of 0.3–2.3 mm). Note that this exponential behaviour must be due to collective grain motion because the bulk modulus of glass is too large to allow such a range of compression.

The results shown in Fig. 1b, c indicate that λ is affected by both the plate size and the stress state at the bottom of the bucket. Although the former can be easily measured, the latter can be quantified only through the measured quantity $F_0 = F_{\text{bulk}}$ (when $z = 0$), as indicated in Fig. 1a. The quantity F_0 is determined by the size of the granular sample, either the depth for small z_{\max} or the bucket width for large z_{\max} when the walls partially support the grains’ weight at the bottom. The combined data indicate that λ is proportional to $\sqrt{F_0/r}$, as shown in Fig. 1d, where a scaling of $\Delta F \rightarrow \Delta F/F_0$ and $z \rightarrow z/\sqrt{F_0/r}$ causes all of the data in Fig. 1b, c to collapse into a single characteristic exponential. This square-root dependence of λ is unexpected, although r and F_0 do correspond to the two relevant length scales for the system.

To interpret these results, it must be considered that the stress applied by a penetrating object propagates non-uniformly through force chains^{5–10} concentrated along rigid internal structures of grains known as ‘jammed’ states^{11,12}. Such states are repeatedly created and collapsed by the object’s motion. The observed exponential length scale is determined by the failure mode of the jammed state, which in turn depends on the nature of the force chains originating from the plate^{5,7,8}. The applied force from the penetrating plate in our experiments propagates through the entire granular sample to its boundary, so the observation of such a clear length scale is surprising.

Detailed modelling (as for fluids¹³) or *in situ* three-dimensional imaging would allow further characterization of the grain dynamics associated with the collapse of the jammed state. Our results indicate, however, that jamming induced by local stress can be considered as a localized phenomenon with

a well-defined extent. As jamming phenomena can be observed in diverse systems from highway traffic to foams to glasses, the possibility exists that such a length scale has more general implications that extend well beyond a finger being pushed through the sand.

Matthew B. Stone, David P. Bernstein, Rachel Barry, Matthew D. Pelc, Yee-Kin Tsui, Peter Schiffer

Department of Physics and Materials Research Institute, Pennsylvania State University, University Park, Pennsylvania 16802, USA
e-mail: schiffer@phys.psu.edu

- Albert, R., Pfeifer, M. A., Barabási, A.-L. & Schiffer, P. *Phys. Rev. Lett.* **82**, 205–208 (1999).
- Yu, H. S. & Mitchell, J. K. J. *Geotech. Geoenviron. Eng.* **124**, 140–149 (1998).
- Peterson, R. W. in *Calibration Chamber Testing: PTProc. First Intl Symp. Calibration Chamber Testing* (ed. Huang, A.-B.) 315–328 (Elsevier, New York 1991).
- Vanel, L. & Clément, E. *Eur. Phys. J. B11*, 525–533 (1999).
- Geng, J. *et al. Phys. Rev. Lett.* **87**, 035506–035509 (2001).
- Liu, C.-H. *et al. Science* **269**, 513–515 (1995).
- Da Silva, M. & Rajchenbach, I. *Nature* **406**, 708–710 (2000).
- Reydellet, G. & Clément, E. *Phys. Rev. Lett.* **86**, 3308–3311 (2001).
- Bouchaud, J. P., Cates, M. E. & Claudin, P. *J. Physique I5*, 639–656 (1995).
- Mueggenburg, N. W., Jaeger, H. M. & Nagel, S. R. *Phys. Rev. E* **66**, 031304–031312 (2002).
- Liu, A. J. & Nagel, S. R. *Nature* **396**, 21–22 (1998).
- O'Hern, C. S., Langer, S. A., Liu, A. J. & Nagel, S. R. *Phys. Rev. Lett.* **86**, 111–114 (2001).
- Vergeles, M., Koblinski, P., Koplik, J. & Banavar, J. R. *Phys. Rev. Lett.* **75**, 232–235 (1995).

Supplementary information accompanies this communication on Nature's website.

Competing financial interests: declared none.

Transgenic mice

Fat-1 mice convert n-6 to n-3 fatty acids

Mammals cannot naturally produce omega-3 (n-3) fatty acids — beneficial nutrients found mainly in fish oil — from the more abundant omega-6 (n-6) fatty acids and so they must rely on a dietary supply¹. Here we show that mice engineered to carry a *fat-1* gene from the roundworm *Caenorhabditis elegans* can add a double bond into an unsaturated fatty-acid hydrocarbon chain and convert n-6 to n-3 fatty acids. This results in an abundance of n-3 and a reduction in n-6 fatty acids in the organs and tissues of these mice, in the absence of dietary n-3. As well as presenting an opportunity to investigate the roles played by n-3 fatty acids in the body, our discovery indicates that this technology might be adapted to enrich n-3 fatty acids in animal products such as meat, milk and eggs.

The *fat-1* gene of *C. elegans* encodes an n-3 fatty-acid desaturase enzyme that converts n-6 to n-3 fatty acids and which is absent in most animals, including mammals^{2,3}. We transferred this *fat-1* gene into mice and raised them alongside wild-type mice maintained on an identical diet that was high in n-6 but deficient in n-3 fatty acids. However, the fatty-acid profiles of the

two groups turned out to be quite different (Fig. 1). The tissues of wild-type animals contain polyunsaturated fatty acids that are mainly (about 98%) n-6 linoleic acid (designated an 18:2 n-6 fatty acid as it has 18 carbon atoms and 2 double bonds, one at position n-6) and arachidonic acid (AA, 20:4 n-6), with very little n-3 fatty acid (from a dietary source). By contrast, the transgenic animal tissues are rich in n-3 polyunsaturated fatty acids, including linolenic acid (18:3 n-3), eicosapentaenoic acid (EPA, 20:5 n-3), docosapentaenoic acid (DPA, 22:5 n-3) and docosahexaenoic acid (DHA, 22:6 n-3).

The concentrations of n-6 linoleic and arachidonic acids in the tissues of the transgenic mice are significantly reduced, indicating that n-6 fatty acids have been converted to n-3, causing the ratio of n-6 to n-3 to drop from 20–50 to almost 1. This n-3 enrichment at the expense of n-6 gives a balanced ratio of n-6 to n-3 and of AA/(EPA+DPA+DHA) in all of the organs and tissues tested (Table 1). Transgenic skeletal muscle contains more EPA than DHA, but DHA is the dominant n-3 fatty acid in other organs.

We have examined the tissue fatty-acid profiles in four generations of transgenic mouse lines (homozygote or heterozygote) and find consistently raised n-3 fatty acids, indicating that the transgene is functionally active *in vivo* and transmittable. The transgenic mice appear to be normal and healthy.

Efforts have been made to incorporate n-3 fatty acids into the food supply^{1,4} because of their health benefits and concern over the high n-6:n-3 ratio in Western diets. Our findings suggest a new strategy for producing food that is enriched in n-3 fatty acids from livestock carrying an n-3 desaturase trans-gene. At present, farm animals are fed fishmeal and other marine products, but this is time-consuming and costly, and is limited by the quantity of the source⁵. Production of n-3 fatty acids by the animals themselves would be a cost-effective and sustainable way of meeting the increasing demand; the ideal n-6:n-3 ratio of about 1 could be achieved by consuming foods

Table 1 Fatty-acid ratios in WT and *fat-1* mice

	n-6/n-3*		AA/(EPA+DPA+DHA)	
	WT	TM	WT	TM
Muscle	49.0	0.7	11.3	0.4
Milk†	32.7	5.7	15.7	2.5
Erythrocyte	46.6	2.9	27.0	1.6
Heart	22.8	1.8	14.3	0.9
Brain	3.9	0.8	3.6	0.7
Liver	26.0	2.5	12.5	0.9
Kidney	16.5	1.7	11.9	1.2
Lung	32.3	2.2	19.8	1.2
Spleen	23.8	2.4	17.3	1.5

Both wild-type (WT) and transgenic (TM) mice were 8-week-old females fed on the diet described in Fig. 1. AA, arachidonic acid (20:4 n-6); EPA, eicosapentaenoic acid (20:5 n-3); DPA, docosapentaenoic acid (22:5 n-3); and DHA, docosahexaenoic acid (22:6 n-3).

*The n-6:n-3 fatty-acid ratio is given by (18:2 n-6 + 20:4 n-6 + 22:4 n-6 + 22:5 n-6)/(18:3 n-3 + 20:5 n-3 + 22:5 n-3 + 22:6 n-3).

†The milk was taken from the stomach contents of 5-day-old neonatal mice born to wild-type or transgenic mothers.

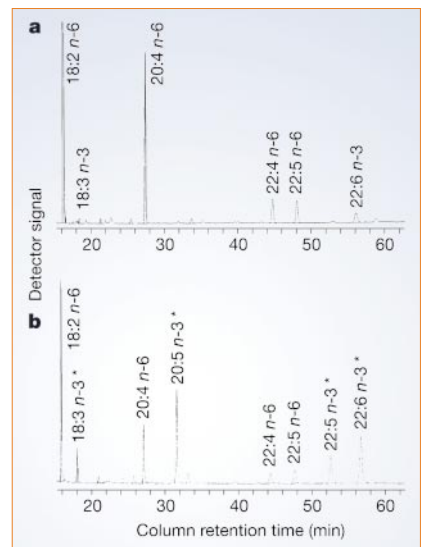


Figure 1 Partial gas chromatograph traces showing the polyunsaturated fatty-acid profiles of total lipid extracted from mouse skeletal muscle. **a**, **b**, Traces from lipid from **a**, a wild-type mouse, and **b**, a *fat-1* transgenic mouse (heterozygote). The expression vector used for microinjection contained the humanized *fat-1* sequence (with modification of codon usage) and a chicken β -actin promoter and cytomegalovirus enhancer, which allow high and broad expression of the transgene in mice^{6,7}. Both the wild-type and transgenic mice were 8-week-old females that were fed on the same diet, which was high in n-6 but low in n-3 fatty acids. The lipid profiles show that concentrations of n-6 polyunsaturated acids (18:2 n-6, 20:4 n-6, 22:4 n-6 and 22:5 n-6) are lower and levels of n-3 fatty acids (asterisks) are markedly higher in transgenic (**b**) than in wild-type (**a**) muscle. (Homozygotes and heterozygotes have a similar phenotype.)

containing this ratio and without introducing stringent dietary changes.

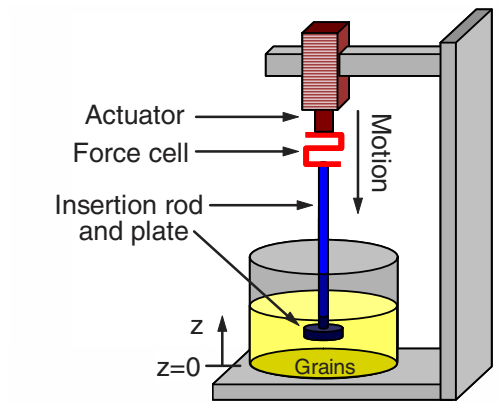
Our transgenic mice also offer a model for investigating the biological functions of n-3 fatty acids and the importance of the ratio of n-6:n-3 in disease prevention and treatment. Specific effects of n-3 fatty acids and of the n-6:n-3 ratio can be tested in different organs and tissues — for example, they may alter gene expression or physiological activity during the life cycle. Our mouse lines could be genetically backcrossed with mouse disease models to test the effects of n-3 fatty acids on the pathogenesis and treatment of those diseases.

Jing X. Kang*, Jingdong Wang*, Lin Wu†, Zhao B. Kang*

Departments of *Medicine and †Dermatology, Massachusetts General Hospital and Harvard Medical School, Boston, Massachusetts 02114, USA
e-mail: kang.jing@mgh.harvard.edu

- Simopoulos, A. P. *et al. (eds) World Rev. Nutr. Diet* Vol. 83 (Basel, Karger, 1998).
- Spychalla, J. P., Kinney, A. J. & Browse, J. *Proc. Natl Acad. Sci. USA* **94**, 1142–1147 (1997).
- Kang, Z. B. *et al. Proc. Natl Acad. Sci. USA* **98**, 4050–4054 (2001).
- Simopoulos, A. P. & Cleland, L. G. (eds) *World Rev. Nutr. Diet* Vol. 92 (Basel, Karger, 2003).
- Naylor, R. L. *et al. Nature* **405**, 1017–1024 (2000).
- Niwa, H., Yamamura, K. & Miyazaki, J. *Gene* **108**, 193–199 (1991).
- Okabe, M. *et al. FEBS Lett.* **407**, 313–319 (1997).

Competing financial interests: declared none.



Supplementary Figure Legend

This figure depicts the granular penetrometer apparatus used for the measurements presented. All data shown were obtained using monodisperse spherical glass beads (Jaygo Inc.) with a packing fraction of $60\pm 3\%$ and $d_{\text{grain}} = 0.92\pm 0.03$ mm. Data were acquired with penetration velocity of $v = 0.5$ mm/sec., container diameter of 210 mm, and vertical disc thickness of 7.6 mm. Data were taken from the top surface ($z \sim z_{\text{max}}$) down to just above the bucket bottom ($z \sim 4$ mm). Measurements were performed at either 50 Hz or 100 Hz and averaged to either 1 mm or 0.5 mm distance intervals to reduce fluctuations. In addition, all the data were averaged from at least 3 to 5 separate penetration runs. In order to obtain a constant packing fraction throughout the sample (necessary for reproducible results), the bucket was filled through a tube which was centered in the bucket and slowly raised such that the grains did not experience free-fall during filling. Equivalent data were also obtained with samples in which the bucket was filled and then the stress state was changed by pulling up through the grains either a thin sleeve which fit just inside the bucket's inner diameter or a mesh through which the grains fell. The sample surface was flattened by the penetration, but there was no perceptible change to the surface after the plate was submerged.